Paper No.
00050

CORROSION 2000

EFFECT OF BUBBLES ON MASS TRANSFER IN MULTIPHASE FLOW

Hongwei Wang, William Paul Jepson
Ji-Yong Cai, Tao Hong and Madan Gopal
NSF, I/UCRC Corrosion in Multiphase Systems Center
Department of Chemical Engineering
Ohio University
Athens, Ohio 45701

Howard Dean Dewald
Department of Chemistry and Biochemistry
Clippinger Laboratories
Ohio University
Athens, Ohio, 45701

ABSTRACT

In multiphase flow, bubbles are produced and collapse on the solid/liquid interface. Bubble collapse can enhance the CO_2 corrosion of carbon steel pipe, as shown by coupon surface analysis, corrosion rate measurements and visualization of bubble movement in multiphase flow.

Using the electrochemical limiting current density technique, experiments have been carried out to study the effect of bubbles on mass transfer in an electrochemical cell and in slug flow. The limiting current density signal as a function of time and frequency shows the direct influence of bubble movement on mass transfer. It also indicates the difference of mass transfer in fully developed turbulent flow, an electrochemical cell and slug flow. The enhancement of mass transfer coefficient by bubble collapse is considered an important factor that contributes to the increased corrosion rate in multiphase flow.

Keywords: slug flow, bubble, cavitation, mass transfer enhancement, CO_2 corrosion, pipe

INTRODUCTION

Flow accelerated corrosion (FAC) has received significant attention recently in various industries, e.g. the carbon steel portion of piping and equipment found in power plants and offshore oil and gas production. FAC results in thinning of piping, vessels, and equipment from the inside. In offshore oil and gas production, multiphase slug flow is a common flow regime. Its unique multiphase turbulence results in the enhanced internal corrosion of carbon steel pipelines. It is well known that mass transport information is key to the overall understanding of flow accelerated corrosion. The FAC corrosion in multiphase flow in particular requires the knowledge of mass transfer characteristics, as this determines the rate-limiting step of corrosion. In multiphase flow, two questions remain unanswered, namely, the effect of bubbles on the mass transfer, and the bubble influence on the corrosion process. The first question will be the main concern of this paper.

Corrosion

Extensive studies of CO_2 corrosion in slug flow have been conducted in the past few years[1-7]. In slug flow, the effects of parameters such as Froude number, slug frequency, water cut, liquid viscosity, gas density, oil type, temperature, pressure and pipeline inclination on CO_2 corrosion have been studied extensively.

The mechanism of corrosion enhancement of slug flow was explained through extensive experimental methods, such as surface analysis of coupons, visualization of slug flow, shear stress, pressure, and mass transfer measurements. The enhancement of corrosion in slug flow was attributed to the impact and subsequent collapse of the gas bubbles as they hit the bottom of the pipe. These pulses of bubbles are generated within the mixing zone of the slug.

Flow

Jepson[8] showed that the turbulence of slug flow is associated with pulses of gas bubbles reaching the bottom surface of the pipe. The gas bubbles trapped in the mixing zone are forced down towards the wall surface, where they are released in the form of pulses of bubbles. The intensity and frequency of these bubbles increase with Froude number.

Gopal and Jepson[9] used digital image analysis techniques in the study of velocity and void profiles in slug flow. Through the visualization of flow, they showed gas bubbles result with a high degree of turbulence, and destroy the hydrodynamic boundary layer within the mixing zone.

Peaks of instantaneous wall shear stress[1, 10] and instantaneous pressure drop[11] in slug flow have been reported, it is believed that these macroscopic peaks are directly related to the frequency of pulses of bubbles in the mixing zone of the slug flow.

Mass Transfer

The mass transfer change under disturbed flow conditions, such as near pits, weld bead, etc. has been examined in the presence of fully developed flow, slug flow and annular flow[12, 13]. The direct comparison of steady state mass transfer coefficients in these situations indicates that the weld bead and pit could increase the mass transfer coefficient and the corrosion rate.

It was also found that slug flow usually results in a higher mass transfer coefficient, which contributes to the high corrosion rate. Jiang[13] reported large limiting current peaks in slug flow and slug-

annular flows and hypothesized their existence as the reason for enhanced corrosion in slug flow. However, the mechanism needs to be investigated further.

In the present work, the electrochemical limiting current density technique has been used as an effective method to study the transient mass transfer resulting from movement of gas bubbles in these electrochemical systems, both in an cell and in slug flow.

MASS TRANSFER ENHANCEMENT MECHANISM

Several studies in ultrasound sonochemistry have investigated the effect of the collapse of gas bubbles on the mass transfer to a solid surface. In view of the similarity between bubble collapse in slug flow and in an ultrasound system, these analyses are collected below.

Birkin et al.[14] studied the important effect of ultrasound on mass transport with a microelectrode. They recorded the current as a function of time at a 25 μm diameter gold microelectrode electrode held potentiostatically at + 600 mV vs. SCE in a methanol solution containing ferrocene (5 mM) and tetra ethyl ammonium tetra fluoroborate Et_4NBF_4 (0.1 M). At this chosen potential, the oxidation of ferrocene was mass transport-controlled. The presence of ultrasound produces microjets due to collapsing/cavitating bubbles directed at the solid-liquid boundary.

It was found in Birkin's[14] work that well resolved current spikes were about two-orders of magnitude higher than the steady state mass transport current produced in the absence of forced convection. They found that increasing the intensity of the ultrasound source or decreasing the separation between the ultrasonic horn and electrode resulted in an increase in the frequency and magnitude of the observed events. They also found that the intensity of the ultrasound wave has an effect on the magnitude of the energetics of the cavitation bubble collapse and density of bubble events. Similarly, slug flow also has an effect on the energetics of the bubble collapse and density of bubble events.

Clear current spikes and decay transients due to a single bubble were observed in earlier works [15, 16]. They have concluded that the events observed, attributed to cavitation events, are not the result of erroneous noise phenomena but only exist if the potential is in the correct region for the redox couple employed. In the same way if the solution is not excited by ultrasound to produce the cavitation events, then no transient events are observed. These observations show that the current transients are the result of cavitation enhanced forced mass transfer.

Birkin et al. [15] attributed these events to the impacts of microjets, caused by the collapse of transient cavitation bubbles, directly above or in the proximity of the microelectrode diffusion field. Hence they proposed a scheme to picture the diffusion field of the microelectrode before, during microject impact and after the cavitation event, as shown in Figure 1. Figure 1(a) shows the hemispherical diffusion field of a microelectrode held at the steady state mass transport limited condition in the absence of forced convection. Figure 1(b) shows the impact and subsequent compression of the diffusion field produced as a result of forced convection due to the microjet impact. After the cavitational event is over, Figure 1(c) shows how the diffusion sphere of the microelectrode will relax back to the non-convective steady state. This relaxation of the diffusion sphere is analogous to a potential step at the same microelectrode from a potential insufficient to oxidize the redox species to a potential sufficient to oxidize the redox species at the mass transport limited condition. This explanation could be used to account for the bubble impact on the electrode in slug flow.

The direct effect of ultrasound on mass transfer can arise due to three major mechanisms. These are acoustic streaming, microstreaming and microjetting. Basically, acoustic streaming arises from attenuation of the sound field within the liquid, resulting in a pressure gradient and subsequent liquid motion. Microstreaming occurs close to a forced oscillating bubble or some other vibrating body. Microjeting occurs when a cavitation bubble collapses asymmetrically next to a solid/liquid interface.

It is also likely that ultrasound can indirectly produce mass transfer effects due to bubble formation or motion within the diffusion field of the electrode. The effect of bubble motion on mass transfer has been studied[17, 18]. The effects of bubbles generated by an acoustic field, like ultrasound, specifically on mass transfer to an electrode have been studied more recently[14, 15, 20, 21]. Jiang[13] only reported the large limiting current peaks found in slug flow and slug-annular flow. However, the effect of bubbles generated by slug flow on mass transfer to an electrode, to our knowledge, has not been studied extensively.

The diffusion response time for the mass transfer coefficient is relatively short (~1.5 μs). However, it is still longer than the estimated duration of the microjet. As the fluid flow decreases, the response time increases and as a result the error between the recorded electrochemical signal and the actual ultrasonic event becomes extenuated.

The effects of ultrasound on the electrode process were also studied using a pseudo-microelectrode with 1 mm diameter[22]. Although some convection current resulting from movements of solution due to cavitation in the bulk of the solution and /or movements of large gas bubbles formed by the so-called stable cavitation cannot be neglected, the largest contribution to the average current density is due to a large number of individual current pulses. Each of these pulses is a consequence of an individual collapse of a cavitation bubble, which takes place in the vicinity of or at the surface of the electrode.

According to Neppiras the maximum bubble radius R_M is not greatly influenced by the size of the nucleus from which the bubbles formed by cavitation originate.[23] The origin of the pulses and their shape can be explained with the results obtained by Plesset and Chapman[24], who studied the collapse of a vapor filled cavity in the neighborhood of a solid boundary by numerical simulation. Their results show that when an initially spherical bubble of radius R_M collapses, the presence of a solid wall causes the formation of a liquid jet directed towards the surface. The velocity of the jet is about 100 m/s, and depends on the liquid density and on the difference between the external pressure and the pressure inside the bubble (vapor pressure). It does not depend on the initial radius R_M of the bubble. But conversely the time of jet duration (several μs) is proportional to R_M and the volume of the jet is proportional to R_M^3.

Since the maximum radius R_M is approximately the same for all the collapsing bubbles, the different amplitudes of the pulses (peak current values) can not be interpreted as different size of bubbles, but as different distances of these bubbles from the electrode. The largest peak current values resulted from the collapse of bubbles formed in direct contact with the electrode surface. The peaks of lower amplitude result from a sufficient decrease of current (i.e. in less than about 1-5 ms) and a more complicated process takes place partly because of superposition of the pulses and partly removal of the former jet solution by the new one. It is shown that the increase of electrolytic current resulting from sonication is not given by an increase of current density at the whole electrode but by a limited number of local individual pulses caused by violent collapses of cavitation bubbles in the neighborhood of the electrode.

Kilma et al.[25] proposed that the limiting current is the sum of steady state and transient components. The increase of the electrolytic current due to sonication is mainly given by the transient component, originated from a series of local individual pulses resulting from jets of solution rather than from a decrease of the diffusion layer thickness due to stirring of the bulk solution. However, other researchers considered this reason in other ways.

Marken et al.[26] stressed the dominating effect caused by ultrasound is the strongly enhanced mass transport resulting from a very thin diffusion layer thickness. He neglected the contribution of a transient component on the limiting current. He summarized the effect of ultrasound on the electrochemical process as follows: i) mass transfer is observed to be strongly enhanced near the electrode surface. Possible processes that contribute to mass transport are acoustic streaming, cavitation or micro streaming at the electrode surface. ii) cavitation has a considerable cleaning effect on the electrode, but also erodes away the surface material. iii) radical species formed in the cavitation event are highly reactive and may participate in the electrode reaction process. iv) ultrasound enhances the rate of certain chemical reactions, such as disproportionations, coupled to the heterogeneous electrode transfer. It was resulted from the extreme condition that when a bubble grows and collapses, high intensity pressure waves are created for a few milliseconds, with the instantaneous local pressure increasing up to 4000 atm with a temperature increase of up to 800 °C. [27]

It has been demonstrated that for the chosen example of heterogeneous electron transfer reactions no obvious direct effect of intense ultrasound on the rate of simple electron transfer processes for fast, quasi-reversible systems exists.[26] The dominating effect caused by ultrasound is the strongly enhanced mass transport resulting from a very thin diffusion layer thickness.

From the view of chemical engineering, the effects of ultrasound and mechanical agitation was compared on a reacting solid-liquid system.[28] When solid particles are in the vicinity of the cavitation bubble the implosion may occur symmetrically or asymmetrically, depending on the proximity of the solids. Symmetric cavitation creates shock waves that propagate to the surrounding solids causing microscopic turbulence and /or thinning of the solid-liquid film. This phenomenon is called microstreaming and is thought to be responsible for increasing the rate of mass transfer through the film. When solid particles are in close proximity to the bubble, it is unable to collapse symmetrically. This is known as asymmetric cavitation and is responsible for the formation of microjets of solvents, which bombard the solid surface, leading to pitting and general corrosion.

Enhancement of ultrasound may be attributed to its chemical or mechanical effects or to both simultaneously. The chemical effects of ultrasound are due to the implosion of microbubbles, generating free radicals with a great propensity for reaction. Mechanical effects are caused by shock waves formed during symmetric cavitation. Hagenson found that the most important of these are that ultrasound increases i) the intrinsic mass transfer coefficient of the liquid reactant through the interfacial film by a factor ~ 2, ii) the effective diffusivity of the liquid reactant through the product layer surrounding the unreacted core by a factor 3.3.

Cooper and Coury[29] observed that voltammetry in the presence of ultrasound using 0.01 M potassium ferrocyanide with a Pt working electrode shows near steady state behavior with large current output that oscillates about a stable, averaged value at mass-transport-limited potentials. Cooper proposed a qualitative model of convective mass transport in sonovoltammetry. The model states that the current signal consists of a time-independent dc component and a time dependent ac component: $m_T = m_{dc} + m_{ac}$.

The dc signal arises from steady forces, primarily acoustic streaming, but it may be affected by the intensity of ultrasonic cavitation. A portion of the ac signal is driven at the ultrasonic frequency, and this signal results from the field-induced fluid oscillation. Another portion of the ac signal does not occur at the frequency of the ultrasound, and this arises from cavitational effects.

Cooper considered that cavitation may produce an overall time-averaged enhancement of mass transport, but the magnitude of this effect varies with the experimental time scale. The data was collected at a sampling frequency of 2~8 kHz.

The process of erosion caused by cavitation was studied to determine the influencing factors.[30] It was found that erosion does not result from the shock wave or microstreaming resulting from the oscillation of bubbles, but is due to the jets created by the asymmetric implosion of cavities, especially those adjacent to the plate and with a radius smaller than 4μm. The erosion of the plate is not mechanical due to the jets, but due to a dissolution of the plate from the continuous renewal of solvent at the point of crash of the jets.

The potential and current oscillation in the reduction of $Fe(CN)_6^{3-}$ ions involving convection mass transfer were addressed recently.[31, 32] It was found that the convection mass transfer, which is induced by hydrogen evolution, plays an important role in the oscillations. It is seen that the convection mass transfer induced by gas bubbles would play an important role in the oscillation of limiting current in the slug flow.

Xia et al. analyzed the influence of attached gas bubbles on corrosion. [33] In many cases, pitting was found at sites where small gas bubbles were attached to the steel surface. It is well known that in chloride solutions pits easily nucleate at the triple gas/liquid/metal boundaries. Initially a crevice around the attached gas bubbles is produced and develops into a pit.

EXPERIMENTAL

Figure 2 shows the 25ml electrochemical cell. The working electrode, reference electrode and auxiliary electrodes are made of nickel. The cross-sectional area of working electrode is 0.072 cm^2. The cell was filled with 20 ml 2N NaOH and 0.01 M potassium ferro/ferricyanide solution. The nitrogen is bubbled through the solution beneath the working electrode through a plastic tube.

The overall layout of the pipe system is shown in Figure 3. The flow loop is a 15 m long 10 cm I.D. plexiglas pipe. A 1.3 m^3 stainless steel tank is filled by 0.85 m^3 electrolyte solution containing 1 N sodium hydroxide and 0.005 M potassium ferro/ferricyanide. Nitrogen gas is stored in a pressurized gas tank and is added into the system through a pressure regulator and a gas flow meter. The system pressure is maintained at 1 atm.

The test section is a 10 cm I.D. plexiglas pipe fitted with flush-mounted electrodes. The orientation of the electrodes in the direction of flow is reference electrode, working electrodes and auxiliary electrode, as shown in Figure 4. The working and reference electrode are made of 1.613 mm diameter Hastelloy C-276 and at equal distance at the bottom. The distance between two consecutive electrodes is 4.5 mm. The auxiliary electrode is a ring Hastelloy C-276 electrode mounted flush with the pipe wall.

The potentiodynamic and potentiostatic curves are obtained using Gamry software CMS 105. The system could record a maximum of 32768 data points per run, and the sampling rate could reach 2000 Hz.

Experiments carried out in electrochemical cell are listed in Table 1. The experiments were also carried out in stationary slug flow, where the Fr number is 4, 5, 6, and 7.

RESULTS & DISCUSSION

Effect of bubble on mass transfer in electrochemical cell

Figure 5 and 6 show the potentiostatic curve and Fast Fourier Transform (FFT) analysis result respectively when the bubbling frequency is 0.2 Hz. Regular peaks at interval of approximately 5 seconds can be seen. The results are also summarized in Table 2. The potentiostatic curve quantitatively represents the transient limiting current density at an applied potential, e.g. –0.4 V. It confirms the relationship between the oscillation and the physical bubble movement. The negative current corresponds to the cathodic current. The $|I_{max}|$ is 4.50e-4 (A/cm^2) corresponds to the condition at which a bubble just detaches from the working electrode. When a bubble attaches to the working electrode for about 5 seconds, the $Fe(CN)_6^{3-}$ ion in the interface film between the electrode and bubble is consumed very quickly, and thus the limiting current density decreases to the lowest value close to zero. When the gas bubble attaches to the surface of the working electrode, the limiting current decreases at different rates based on the duration of bubble attachment. The diffusion sphere of the electrode will relax back to the non-convective steady state after the bubble impact event is over, as shown in Figure 1. This relaxation of the diffusion sphere is analogous to a potential step at the same electrode from a potential insufficient to reduce the redox species to a potential sufficient to reduce the redox species at the mass transport limited condition. When the bubble detaches from the electrode again, the concentration of $Fe(CN)_6^{3-}$ ion is renewed, and limiting current reaches the peak value.

Through Fast Fourier Transform analysis, it can be seen from Figure 6 that the dominant frequency occurs at 0.15 Hz and is close to the 0.2 Hz bubbling frequency. The frequency f1 shown in Table 2 therefore represents the bubbling frequency, f2 and f3 are second and third harmonics respectively.

The results for 0.03 Hz of bubbling test are shown in Table 2. Figure 7 and Figure 8 represent the results at 0.03 Hz bubbling in cell. It is also seen that the dominant frequency at 0.033 Hz is close to the 0.03 Hz bubbling frequency. It is seen from Figure 7 that between the time interval of 30 to 60 seconds, four continuous peaks are seen. The peaks are associated with the phenomenon that the first four small gas bubbles attach to the working electrode and coalesce to a single and larger bubble on the surface of working electrode. When the fifth bubble further attaches to the big bubble, the large internal pressure thins the diffusion layer and the current decreases to the lowest value close to zero because of the complete consumption of $Fe(CN)_6^{3-}$ ion in the boundary layer. Until the ninth bubble attaches to the surface of the working electrode, the current stays very close to zero. When the ninth bubble attaches to the electrode, the whole bubble detaches from the electrode. The cycle of oscillation repeats itself.

Table 3 compares the basic nature of bubble movement in the cell vs. slug flow. In the cell, a bubble slowly collapses on the surface of the electrode. However, bubbles could quickly collapse in slug flow. Because of the short duration of collapse in slug flow, the current can hardly decrease to a very low value. The microjet and microstreaming effects are considered to be effective in slug flow and contribute to the mass transfer enhancement.

Effect of bubble on mass transfer in slug flow

Figure 9, 11, 13, 15, show the results of limiting current density measurements in stationary slug flow at Fr number 4, 5, 6 and 7 respectively. The sampling rate is 50Hz.

Comparison of Figure 9, 11, 13 and 15 shows that the number of spikes and the magnitude all increase with the increase of Froude number which represents the turbulence of slug flow. For example, in Froude number 4 shown in Figure 9, only few of spikes exist and the peak value of limiting current density is 0.0095 A/cm^2. In Froude number 6, many more spikes appear and the peak value has reached 0.08 A/cm^2, which is about a 8.4 times enhancement compared to that at Froude number 4. Hence the different amount and magnitude of the limiting current density spikes could directly indicate the relation between physical phenomenon of bubble movement and mass transfer enhancement, considering the conclusion drawn from the electrochemical cell experiments. In lower Fr slug flow, fewer bubbles touch to bottom, whereas more and more can touch and collapse on the bottom of the pipe at higher Fr slug flow.

Based on the present data acquisition method, these spikes never appear in full pipe flow where no bubbles exist. The fluctuation of limiting current density in full pipe flow would follow the base line in Figure 9. Hence, such large limiting current density spike becomes a footprint to detect the existence of bubbles collapsing on the bottom of a pipe in multiphase flow, e.g. slug flow, bubbly flow.

Figure 10, 12, 14, 16 show the corresponding signal as a function of frequency. It can also be seen that the amplitude gradually increases with the increase of Froude number.

The amplitude of peak value represents the energy level of bubbles in slug flow. It can be assumed that three kinds of bubbles exist. Above some high energy level, the bubbles can collapse on the bottom surface of a pipe, and completely destroy the mass transfer boundary layer. Immediately after this event, the electrode experiences a surge in electrolyte concentration approaching bulk concentration, which greatly increases the mass transfer rate. This process is related with microjetting, which occurs when a bubble collapses asymmetrically next to a solid/liquid interface. At the intermediate energy level of bubbles, the gas bubble can enter the mass transfer boundary layer, but does not collapse on the wall because of lower energy. This process could be related with microstreaming, which occurs close to forced oscillating bubbles or some other vibrating body, e.g. a small oil droplet. At the low energy level, the gas bubble can not enter the mass transfer boundary layer and its direct influence on mass transfer is negligible. However it can produce turbulence and further influence the pressure gradient and wall shear stress. In the slug flow with different Froude number, these three kinds of bubbles can co-exist. In addition, the distribution of these bubbles is closely related to the change of Froude number or intensity of slug flow.

It has been found in the pressure drop measurement in slug flow that the dominant frequency occurs at about 5 Hz.[11] This dominant frequency is associated with the frequency of pulses of bubbles in the mixing zone of slug flow. The dominant frequency of 5 Hz is apparent in Figure 10, 12, 14, 16. In this manner the mass transfer study provides a tool to detect the bubble hydrodynamics in multiphase flow.

The effect of the viscosity of oil on corrosion in three-phase flow has been studied previously.[3] Oils with 2 cp and 96 cp have been used in experiments. The water cut ranged from 0 to 100 %. It was found that the oil with low viscosity entrains more gas in the slug than the higher viscosity oil. The pressure drop across the slug is larger for the higher viscosity oil. It was also found that the corrosion

rate in 96 cp oil/water mixture is higher than in 2 cp oil/water mixture in slug flow. In the study of cavitation pitting and erosion of aluminum 6061-T6 in mineral oil and water, it was found that the cavitation effect is stronger in higher viscosity liquid.[34] Hence, it is concluded that higher liquid viscosity and higher cavitation increase the corrosion rate. Thus it is derived that a cavitation type phenomenon probably exists in slug flow. Furthermore, the bubble effect on mass transfer in slug flow could be confirmed again by above phenomena, considering the known mechanism of bubble effect by ultrasound and cavitation.

CONCLUSIONS

- Ultrasonic sonochemistry studies have shown the effect of collapsing gas bubbles on instantaneous mass transfer rates. The schematic model (Birkin et al. 1996) could be used to explain the effect of bubbles in slug flow and in an electrochemical cell.
- The experiments in the electrochemical cell confirm the relationship between the oscillation of the limiting current and the physical bubble movement. It further proves that the electrochemical method can be used to study the bubble movement and its effect on mass transfer. Therefore, it could be used to study the transient mass transfer in slug flow, which is critical to understand the corrosion process in slug flow.
- Comparison of limiting current density in full pipe flow and slug flow indicated that the existence of bubble effects in slug flow and its contribution to mass transfer.
- Peak value of limiting current density in slug flow is considered, to our knowledge, to be able to partially represent the mass transfer enhancement by bubbles in slug flow. Such mass transfer enhancement composes an important factor by which slug flow causes the enhancement of corrosion rates.

Currently the mass transfer correlation in slug flow is being developed. This is expected to provide further understanding of flow effect on CO_2 corrosion in slug flow.

ACKNOWLEDGMENTS

Author would like to thank Dr. P. R. Birkin (University of Southampton, England), Dr. S. Zhou (Xiamen University, China) and Dr. R. E. Apfel (Yale University) for helpful discussion. Thanks also go to Mr. A. Krebs' direct guide to application of Gamry software. Financial support was received from the advisory board companies of the Corrosion in Multiphase Systems Center. Also, a graduate fellowship from Texaco for Hongwei Wang is gratefully acknowledged.

REFERENCES

1. Sun, J. Y., and Jepson, W. P., "Slug Flow Characteristics and Their Effect on Corrosion Rates in Horizontal Oil and Gas Pipelines", 67th Annual Technical Conference and Exhibition of the Society of Petroleum Engineers, 1992, P215
2. Zhou, X. and Jepson, W. P., 1994, "Corrosion in Three-Phase Oil/Water/Gas Slug Flow in horizontal Pipes", Corrosion/94, Paper no. 26, (Baltimore, MD, NACE International, 1994)
3. Jepson, W. P. and Menezes, R., 1995, "The Effects of Oil Viscosity on Sweet Corrosion in Multiphase Oil, Water/ Gas Horizontal Pipelines", Corrosion/95, paper no. 106, (New Orleans, LA, NACE International 1995)
4. Gopal, M., Kaul, A., and Jepson, W. P., 1995, " Mechanisms Contributing to Enhanced Corrosion in Three Phase Slug Flow in Horizontal Pipes", Corrosion/95, paper no. 105, (New Orleans, LA, NACE International 1995)
5. Kang, C., Wilkens, R., and Jepson, W. P., 1996, "The Effect of Slug Frequency on Corrosion in High Pressure, inclined Pipelines", Corrosion/96, Paper no. 20, (Denver, CO, NACE International 1996)
6. Jepson, W. P., Stitzel, S., Kang, C., and Gopal, M., 1997, "Model for Sweet Corrosion in Horizontal Multiphase Slug Flow", Corrosion/97, Paper no. 11, (New Orleans, LA, NACE International 1997)
7. Jepson, W. P., Krishnamoorthy, V., and Gopal, M., 1998, "Modelling of Multiphase Slug Flow Characteristics and Their influence on Corrosion in Large Diameter, High Pressure Horizontal Pipelines", NACE Middle East Conference, Bahrain.
8. Jepson, W. P., "The Flow Characteristics in Horizontal Slug Flow," 3rd International Conference on Multiphase Flow, 1987, Paper F2, 187
9. Gopal, M., Jepson, W. P., "Development of Digital Image Analysis Techniques for the Study of Velocity and Void Profiles in Slug Flow", International J. Multiphase Flow, 23 (1997) 945.
10. Zhou, X. and Jespon, W. P., "Experimental Study of Slug Flow Characteristics in Horizontal, Multiphase Flows", Proceedings of the Third International Offshore and Polar Engineering Conference, (Singapore, 1993)
11. Maley, L., "Slug Flow Characteristics and Corrosion Rates in Inclined High Pressure Multiphase Flow Pipes", M.S. Thesis, Ohio University, 1997
12. Xie, Q. Q., "Study on Mass Transfer and Turbulence in Large Pipe Flow Using Limiting Current Density Technique", M.S. Thesis, Ohio University, 1997
13. Jiang, L., Gopal, M., "Multiphase Flow-enhanced Corrosion Mechanisms in Horizontal Pipelines", J. Energy Resources Tech., 120 (1998) 67-71
14. Birkin, P. R., Silva-Martinez S., "The Effect of Ultrasound on Mass Transfer to a Microelectrode", J. Chem. Soc. Chem. Commun., 1995, 1807-1808.
15. Birkin, P. R., Silva-Martinez S., "A Study of the Effect of Ultrasound on Mass Transfer to a Microelectrode", J. Electroanal. Chem. 416 (1996) 127-138.
16. Ben Youssef, A., Haebel, U., Javet, P., "Local Enhancement of Liquid-to-wall Mass Transfer by a Single Gas Bubble", J. Applied electrochemistry, 24 (1994) 658-665.
17. Shah, A., Jorne, J., "Mass Transfer under Bubble-Induced Convection in a Vertical Electrochemical Cell", J. Electrochem. Soc., 136 (1989) 144.
18. Shah, A. Jorne, J., "Mass Transfer under Combined Gas Evolution and Forced Convection", J. Electrochem. Soc., 136 (1989) 153.
19. Whitey, G. M. and Tobias, C. W., "Mass Transfer Effects of Bubbles Streams Rising Near Vertical Electrodes", AIChE J., 34 (1988), 1981-1995
20. Birkin, P. R., Silva-Martinez S., "A Study on the Effect of Ultrasound on Electrochemical Phenomena", Ultrasonic Sonochemistry, 4 (1997) 121-122.

21. Birkin, P. R., O'Connor R., Rapple, C., and Silva-Martinez, S., "Electrochemical Measurement of Erosion from Individual Cavitation Events Generated from Continuous Ultrasound", J. Chem. Soc. Faraday Trans., 94 (1998) 3365-3371.
22. Klima, J., Bernard, C., Degrand, C., "Sonoelectrochemistry: Effect of Ultrasound on Voltammetric Measurements at a Solid Electrode", J. Electroanal. Chem., 367 (1994) 297-300.
23. Neppiras, A. E., Phys. Rep., (Rev. Sect. Phys. Lett.), 61 (1980) 159.
24. Plesset, M. S., and Chapman, R. B., J. Fluid Mech., 47 (1971) 283.
25. Klima, J., Bernard, C., Degrand, C., "Sonoelectrochemistry: Transient Cavitation in Acetonitrile in the Neighbourhood of a Polarized Electrode", J. Electroanal. Chem., 399 (1995) 147-155.
26. Marken, F., Eklund, J. C., Compton, R. G., "Voltammetry in the Presence of Ultrasound: Can Ultrasound Modify Heterogeneous electron Transfer Kinetics", J. Electroanal. Chem., 395 (1995) 335-339
27. Douglas, J. F., Gasiorek, J. M., and Swaffield, J. A., Fluid Mechanics, Pitman Publishing Limited, 1979, 648.
28. Hagenson, L. C., Doraiswamy, L. K., "Comparison of the Effects of Ultrasound and Mechanical Agitation on a Reacting Solid-liquid System", Chem. Eng. Sci. 53 (1998) 131-148.
29. Cooper, E. L., Coury, L. A., "Mass Transfer in Sonovoltammetry with Evidence of Hydrodynamic Modulation from Ultrasound", J. Electrochem. Soc., 145 (1998) 1994-1999.
30. Stephanis, C. G., Hatiris, J. G., Mourmouras, D. E., "The Process (Mechanism) of Erosion of Soluble Brittle Materials Caused by Cavitation", Ultrasonics Sonochemistry, 4 (1997) 269-271.
31. Li, Z. Cai, J., Zhou, S., "Current Oscillation in the Reduction or Oxidation of Some Anions involving Convection Mass Transfer", J. Electroanal. Chem., 436 (1997) 195-201
32. Li, Z., Cai, J., Zhou, S., "Potential Oscillation during the Reduction of $Fe(CN)_6^{3-}$ Ions with Convection Feedback", J. Electroanal. Chem., 432 (1997) 111-116.
33. Xia, Z., Chou, K. –C., and Szklarska-Smialowska, Z., " Pitting Corrosion of Carbon Steel in CO_2 – Containing NaCl Brine," Corrosion, 45, 8, 1989, P636.
34. Rao, B. C. S. and Buckley, D. H., "Cavitation Pitting and Erosion of Aluminum 6061-T6 in Mineral Oil and Water," NASA-TP-2146, 1983

TABLE 1 TEST MATRIX FOR BUBBLE STUDY IN ELECTROCHEMICAL CELL

Frequency of single bubble (Hz)	0.2	0.03
Electrode	Nickel	
Gas	Nitrogen	
Solution	2 N NaOH, 0.01 M $K_4Fe(CN)_6$ and 0.01 M $K_3Fe(CN)_6$	
Temperature (°C)	20 ± 1	

TABLE 2 RESULTS OF BUBBLE STUDY IN ELECTROCHEMICAL CELL

Frequency (Hz)	0.2	0.03
Potentiostatic	Figure 5	Figure 7
FFT	Figure 6	Figure 8
$\lvert I_{max} \rvert$ (A/cm^2)	4.50e-4	8.25e-4
$\lvert I_{min} \rvert$ (A/cm^2)	0	0
FFT, f1 (Hz)	0.15	0.033
FFT, f2 (Hz)	0.3	0.073
FFT, f3 (Hz)	1.13	0.106

TABLE 3 COMPARISON OF BUBBLE IN CELL AND SLUG FLOW

	Energy	Physical phenomena	Mechanism
Cell	Low	Block the surface of electrode (there is still liquid at the interface of bubble and electrode surface, however the redox reaction is quickly finished and the current decreases to zero because of long duration of bubble) and renew the solution around the electrode surface after bubble moves away.	Very slow collapse
Slug flow	Distribution of bubbles with three kinds of energy levels	Quick collapse on the surface of electrode (there are still liquid at the interface of bubble and electrode surface, however the redox material can not be consumed because of short duration of collapse and the current can hardly decrease to very low value close to zero) and renew the solution around the electrode surface after it moves away.	i) Microjet resulting from bubble collapse. ii) Microstreaming

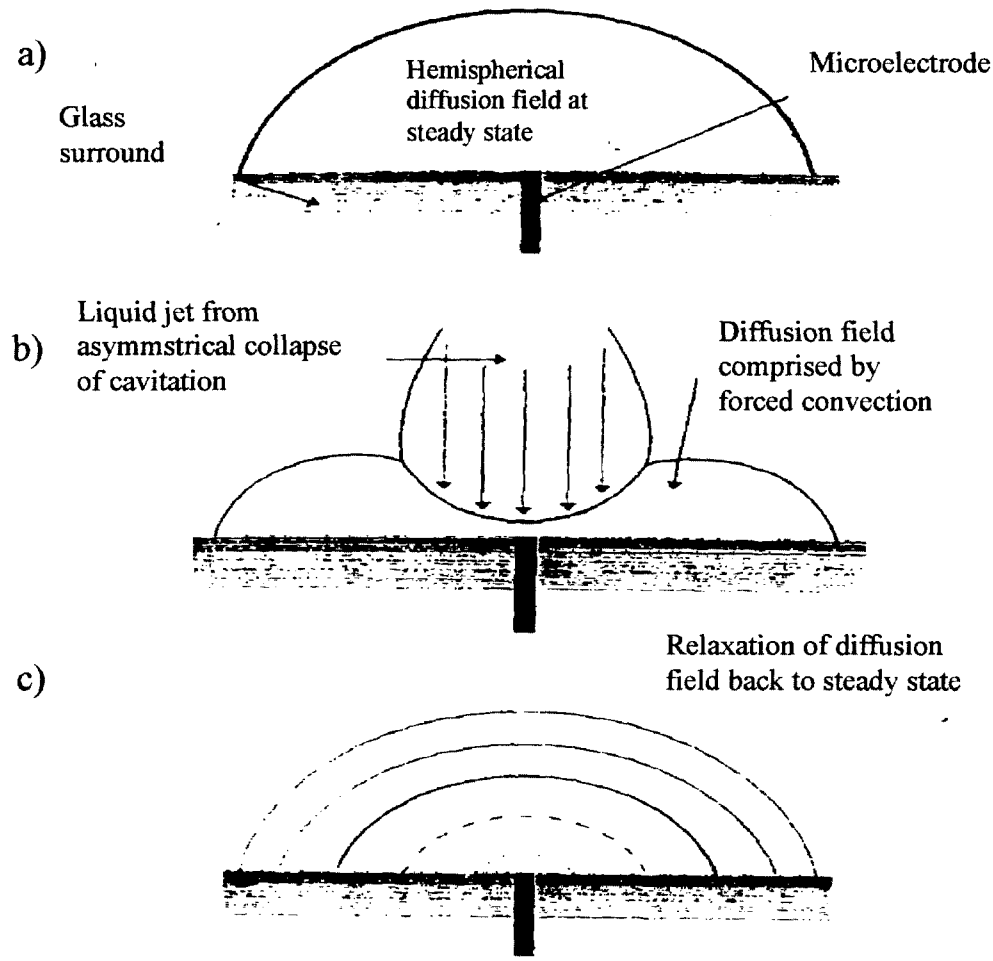

Figure 1 Schematic model of the proposed sequence of events. (a) The diffusion field at equilibrium prior to the caviatation event. (b) The impact of a microjet as a result of asymmetric collapse of a cavitation bubble over the electrode surface. (c) The relaxation of the diffusion field after the cavitation event is over.

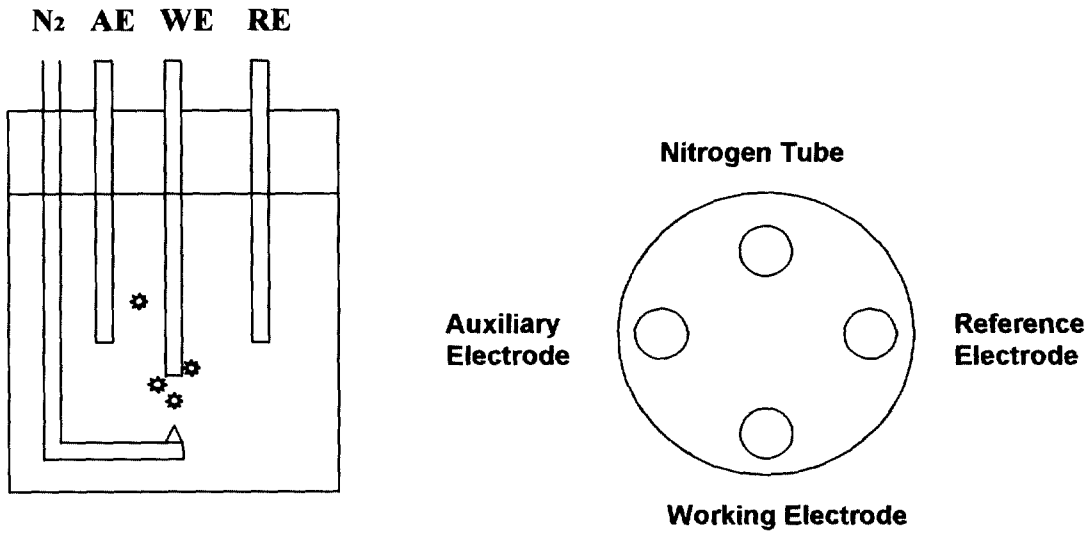

Figure 2 Schematic of electrochemical cell

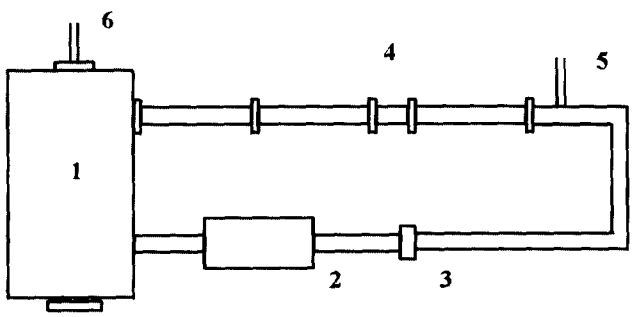

1. Tank
2. Pump
3. Orifice Plate
4. Test Section
5. Gas Feed in
6. Gas Vented

Figure 3 System layout

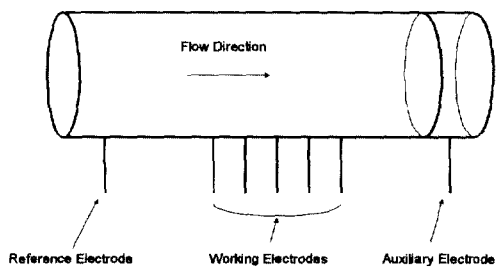

Figure 4 Test section layout

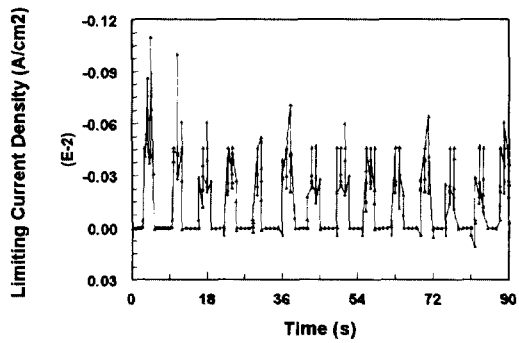

Figure 5 Instantaneous limiting current density for 0.2 Hz bubble in electrochemical cell

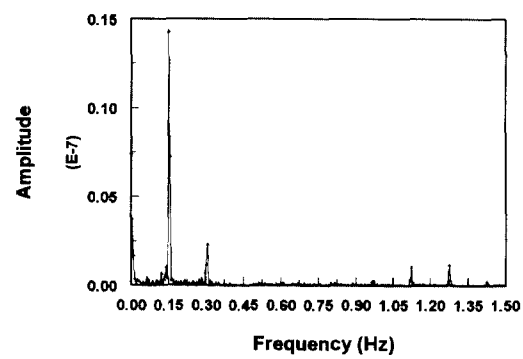

Figure 6 Power spectrum of signal in Figure 5

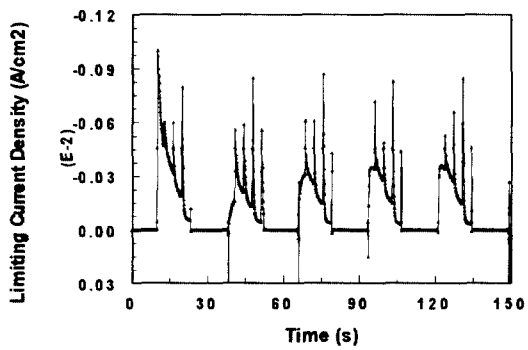

Figure 7 Instantaneous limiting current density for 0.03 Hz bubble in electrochemical cell

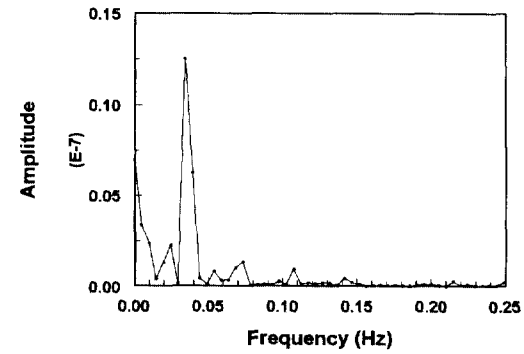

Figure 8 Power spectrum of signal in Figure 7

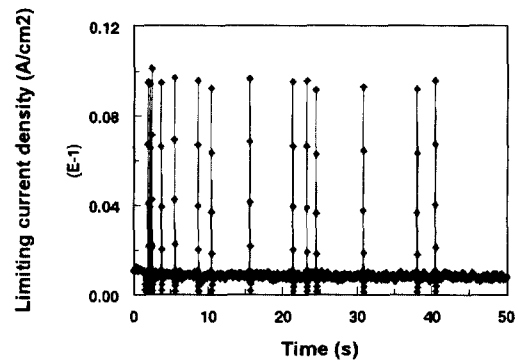

Figure 9 Instantaneous limiting current density in stationary slug with Fr 4.

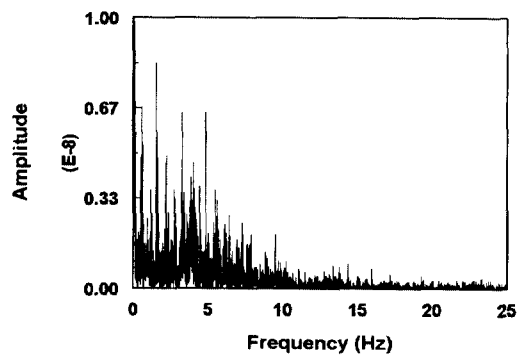

Figure 10 Power spectrum of signal in Figure 9

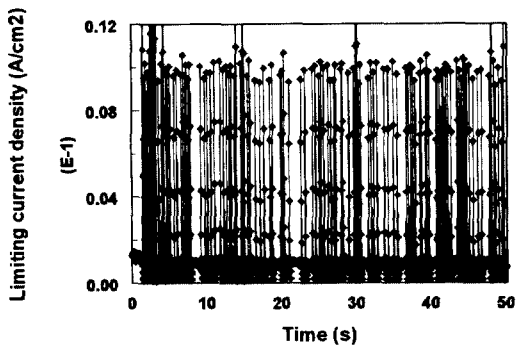

Figure 11 Instantaneous limiting current density in stationary slug with Fr 5

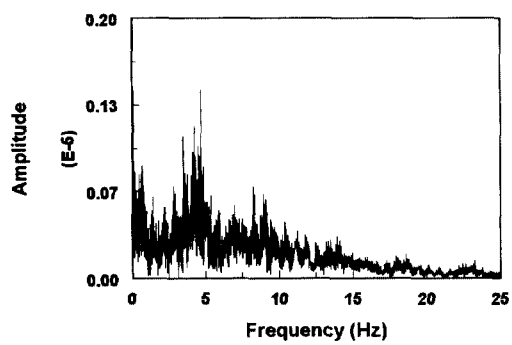

Figure 12 Power spectrum of signal in Figure 11

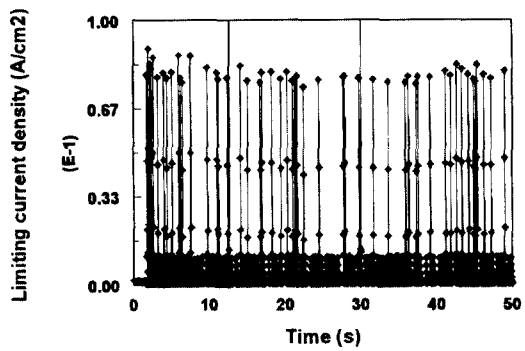

Figure 13 Instantaneous limiting current density in stationary slug with Fr 6.

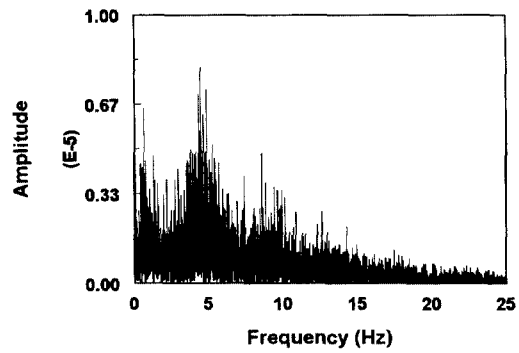

Figure 14 Power spectrum of signal in Figure 13

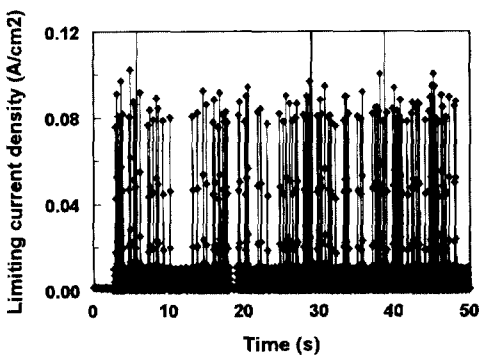

Figure 15 Instantaneous limiting current density in stationary slug with Fr 7.

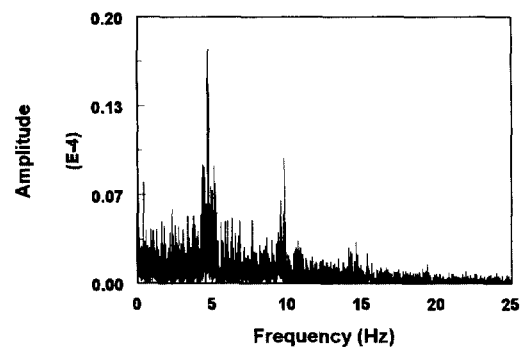

Figure 16 Power spectrum of signal in Figure 15